Applied Surface Science 414 (2017) 238–243

Contents lists available at ScienceDirect

Applied Surface Science

journal homepage: www.elsevier.com/locate/apsusc

Full Length Article

One-step synthesis of nitrogen-doped carbon nanodots for ratiometric pH sensing by femtosecond laser ablation method

Huanhuan Xu[a], Lihe Yan[a,*], Vanthan Nguyen[a,b], Yang Yu[a], Yanmin Xu[a]

[a] Key Laboratory for Physical Electronics and Devices of the Ministry of Education and Shaanxi Key Lab. of Information Photonic Technique, School of Electronics and Information Engineering, Xi'an Jiaotong University, Xi'an 710049, China
[b] Le Quy Don Technical University, Hanoi 122314, Viet Nam

ARTICLE INFO

Article history:
Received 3 January 2017
Received in revised form 17 March 2017
Accepted 12 April 2017
Available online 13 April 2017

Keywords:
Femtosecond laser ablation
Carbon nanodots
Biosensing
Surface states

ABSTRACT

Nitrogen-doped carbon nanodots (CDs) are synthesized by one-step femtosecond laser ablation of graphite powder in aminotoluene at room temperature. The as-prepared CDs have the average diameter of 2.87 nm and possess an excitation-independent emission covering nearly the whole visible light region at a single excitation wavelength. The X-ray photoelectron spectroscopy (XPS) and Fourier transform infrared spectroscopy (FTIR) analysis indicate that there are a huge number of multiple oxygen groups and amine groups on the surface of the CDs. As their different fluorescence peaks originated from different emission surface groups on the nanodots show different pH dependence, these CDs can be used for ratiometric pH sensing.

1. Introduction

Recently, there is a growing interest in developing nanomaterials with sensing capabilities in various fields like diagnostics, drug delivery and environmental monitoring. Accordingly, a variety of nanomaterials with various sensing strategies has been proposed to achieve these goals. Since the pH variation plays a very important role in a broad range of applications from environmental to industrial and biomedical systems, monitoring the pH level is thus crucial to advancing our understanding of cell biology. Thus, great efforts have been made to develop ratiometric fluorescent pH sensors, and a number of fluorescent nanosensors, based on silicon, polymers, or quantum dots have been designed to quantify the pH [1–5]. The ratiometric sensors can provide an internal standard and avoid many interfering potentials, as compared to the single intensity based sensors. However, most of the reported ratiometric fluorescence-based pH nanosensors can only report the pH value of in certain cells due to the large size or limited biocompatibility. Hence, smaller size and more biocompatible materials would be desirable.

As a novel carbon-based nanomaterial with sizes below 10 nm, carbon nanodots have gradually become a rising star in the nanocarbon family since they were firstly discovered in 2004 by purifying single-walled carbon nanotubes through preparative electrophoresis [6,7]. Carbon nanodots have attracted increasing attention owing to their strong fluorescence and they are referred to as fluorescent Carbon. Compared with fluorescent dye molecules and semiconductor quantum dots, fluorescent Carbon nanodots have widely acknowledged advantageous properties such as stable photoluminescence (PL), low cytotoxicity, excellent biocompatibility and easy surface modification, etc. [8–11]. As a result, much attention has also been paid to their potential applications in fluorescent probes, biological labeling, bioimaging and drug delivery [12–14].

So far, many synthetic methods for CDs with tunable size including electrochemical synthesis, hydrothermal oxidation, acidic oxidation, microwave, plasma treatment have been proposed. However, most of the current synthesis methods, such as the chemical and thermal methods, involve toxic chemical reagents or complicated processes, which can be toxic and limit the applications of the products. Furthermore, preparation of surface functionalized nanomaterials usually needs two steps, including the preparation and functionalization processes, which is often complicated and stringent. Since its appearance, femtosecond laser has found many applications in many areas such as ultrafast imaging, micro-structure fabrication and nonlinear spectroscopy due to its unique properties of ultra-short pulse duration and ultra-high peak power [15–18]. Femtosecond laser ablation in solution (FLAS) method can supply a simple alternative to prepare CDs with different fluorescence properties by ablating the reactant carbon source

* Corresponding author.
E-mail address: liheyan@mail.xjtu.edu.cn (L. Yan).

http://dx.doi.org/10.1016/j.apsusc.2017.04.092
0169-4332/

in different solutions. In the synthesis process, ionization of the carbon source and solution occurs and plasma with high temperature and high pressure is formed. Under these extreme conditions, carbon nanoparticles (NPs) with size of several nanometers can be produced, and the surface functionalization on NPs takes place simultaneously [19,20]. By controlling the nature of the solutions, preparation of specific surface functionlized CDs can be achieved in one step.

In this paper, we present a one-step and green route to synthesize nitrogen-containing CDs by pulsed laser ablation in liquid at room temperature. It is found that the CDs are fairly stable, water-soluble and have a strong fluorescence consisting of a dual-band luminescence peak. Structural characterizations and spectroscopic analyses verify that C=O and C=N related surface defects, are responsible for the wide-band fluorescence of the carbon dots. As the different luminescence peaks originate from different functional groups on the CDs and showed different pH dependences, the as prepared CDs can offer a ratiometric sensing platform for the detection the pH value of solutions.

2. Experimental

2.1. Chemicals

Aminotoluene was purchased from Sinopharm Chemical Reagent Co., Ltd. Graphite powder and Cellulose ester Dialysis membranes used for dialysis was purchased from Aladdin Chemistry Co., Ltd (China). The different pH values of the solution were prepared by titrating the sulfuric acid with the sodium hydroxide solution to desired pH values.

2.2. Synthesis of CDs

The CDs were synthesized by one-step femtosecond laser ablation of graphite powders in aminotoluene at room temperature. In a typical procedure, 0.1 mg of graphite powder with a mean size of 400 nm was dispersed into 50 ml of aminotoluene liquid. Then 10 ml of suspension was put into a glass beaker for laser ablation. A Ti: sapphire femtosecond laser system with central wavelength of 800 nm, pulse duration of 150 fs and repetition rate of 1 kHz was used. The laser beam was focused into the suspension by a 100 mm lens for 2 h. The laser power was varied from 100 mW to 400 mW. During the laser ablation, a magnetic stirrer was used to prevent the suspended powders from gravitational settling in the solvent. After laser ablation, large graphite particles were removed by centrifuging the dispersion at 10,000 rpm for 10 min. The obtained solution containing CDs was dialyzed against deionized water before used for pH detection in a dialysis bag (membrane molecular weight cutoff ~1000) for 12 h to remove some impurities.

2.3. Instrumentation

Transmission electron microscopy (TEM) and high resolution transmission electron microscopy (HRTEM) images were carried out on a JEM-ARM200F microscope. Samples were prepared by dropping suspensions of the CDs in water onto Cu TEM grids coated with a holey amorphous carbon film, followed by solvent evaporation in a dust protected atmosphere. UV-2600 spectrophotometer (Shimadzu) was employed to record the UV–vis absorption spectra. The Fourier transform infrared spectroscopy (FTIR) was performed on VERTEX 70 (Bruker). Samples were prepared by dropping suspensions of the CDs in ethanol onto highly pure potassium bromide tabletting, followed by solvent evaporation in a dust protected atmosphere. The measurements of fluorescence spectra were recorded on a FLS920 spectrometer (Edinburgh). X-ray photoelectron spectroscopy (XPS) data for C 1s of the N-CDs solution was measured by an AXIS ULtrabld XPS system. Samples were prepared by dropping suspensions of the CDs in ethanol onto Samples were prepared by dropping suspensions of the CDs in ethanol onto a Silicon substrate, followed by solvent evaporation in a dust protected atmosphere.

3. Results and discussion

3.1. Characterizations of CDs

First, the characterizations of CDs were carried out by TEM, XPS and FTIR analysis. The laser power used for the synthesis of CDs was adjusted to be 400 mW. As shown by the TEM image in Fig. 1(A), the as-prepared CDs distributed on the copper grid homogeneously, and no large aggregations could be observed, indicating that the CDs were well dispersed in water. Fig. 1(B) shows the size distributions of the CDs, in which the sample showed a narrow size distribution with the mean size of about 2.87 ± 0.02 nm. The high resolution TEM image shown in Fig. 1(C) displays a lattice spacing distance of 0.25 ± 0.001 nm, which was in close match with the (020) lattice spacing of graphite [21,22].

The functional groups and chemical structure of the CDs were characterized by FTIR and XPS, respectively. The FTIR spectra of the CDs prepared using different laser power radiation are given in Fig. 2. The absorption bands at 3360 cm^{-1} are attributed to the stretching vibrations of N—H, indicating that N atoms were effectively doped into the CDs. There are also stretching and bending vibrations of CH_2 and CH_3 at around 2920, 2850 cm^{-1} and 1460, 1384 cm^{-1} [21]. The absorption bands at 1544 cm^{-1} and 1634 cm^{-1} correspond to the stretching vibrations of C=C and C=O [23,24]. The FTIR results confirmed that the surface of the CDs is mainly covered with hydroxyl, carboxyl and amino groups. In addition, by comparing the FTIR spectra of CDs prepared using different laser power, we found that the absorption bands from 1220 cm^{-1} to 1720 cm^{-1} and around 3360 cm^{-1} increased with increasing the laser power, indicating that more functional groups were formed on the CDs when the laser power was increased.

More information about the chemical structure of the CDs is explored by XPS analysis given in Fig. 3. The XPS full scan spectrum shows three peaks at 284.74, 398.80 and 532.67 eV, which are attributed to C1s, N1s and O1s (Fig. 3(A)), respectively [24]. The results of the XPS demonstrate that these CDs are mainly composed of C, N and O elements, ant the relative percentages of the corresponding elements are estimated to be about 83%, 3% and 14%, respectively. The high resolution C1s spectra (Fig. 3(B)) can be deconvoluted into three peaks with binding energies at 284.6, 286.7 and 287.6 eV, corresponding to C—C, C—N and C=O, respectively [25,26]. In the deconvoluted O1s spectrum (Fig. 3(C)), two peaks at 531.3 and 533.8 eV reveal the presence of C=O and C—OH/C—O—C [27]. The deconvolution of the N1s spectra (Fig. 3(D)) indicates the presence of C—N—C (399.1 eV) and N—$(C)_3$ (400.8 eV) [28,29]. Consistent with the analysis of FTIR spectrum, the XPS spectrum also confirm that there are a huge number of multiple oxygen and amine groups on the surface of the CDs. Obviously, the surface hydrophilic groups could make the CDs exist steadily in aqueous solution.

3.2. Optical properties of the CDs

In order to explore the optical properties of the CDs, their UV–vis and PL spectra are given in Fig. 4. In the UV–vis spectrum (Fig. 4(A)), there is an obvious optical absorption peaks at 264 nm with an edge extending to around 290 nm. The peak at 264 nm is typically ascribed to the $\pi \rightarrow \pi^*$ transition of aromatic sp^2 domains, while the absorption edge around 290 nm can be attributed to n-π^* transition, which is related to both doping and surface func-

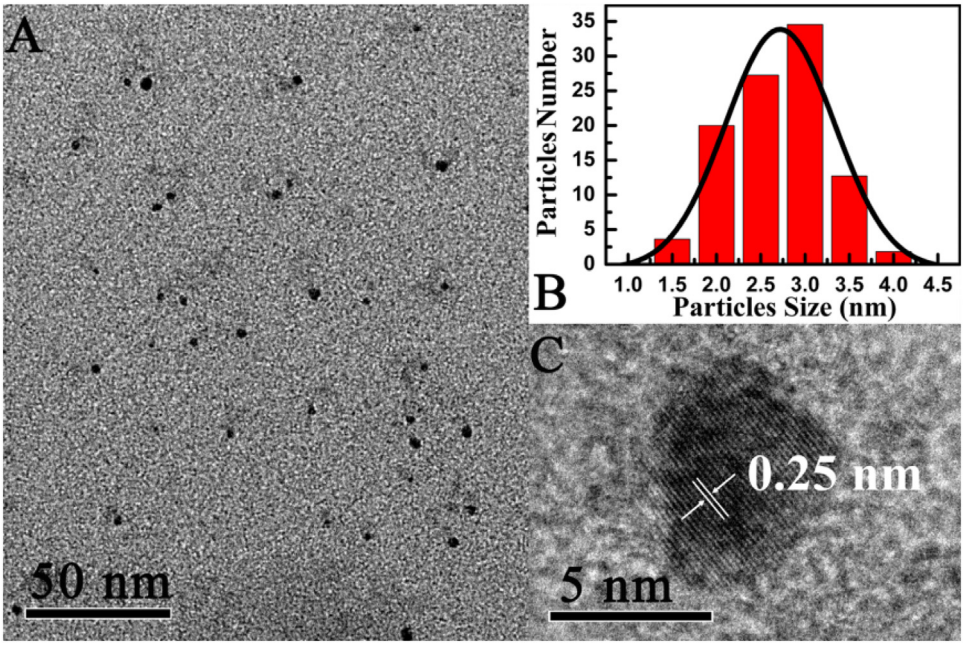

Fig. 1. (A) TEM images of the as prepared CDs, (B) the corresponding size distributions of the CDs, and (C) the HRTEM images of the CDs.

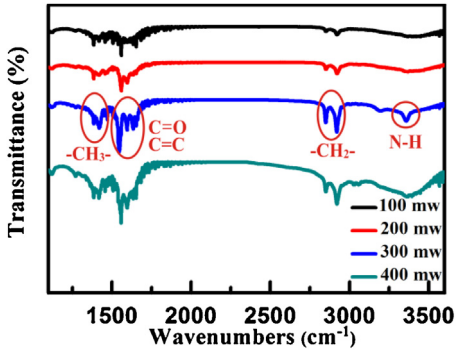

Fig. 2. FTIR spectra of B-C dots and the CDs.

tionalization at the carbon core edge [21,24]. In the fluorescence spectra (Fig. 4(B)), a strong fluorescence emission spectrum centered at 543 nm is observed when excited at 380 nm. The full width at a half maximum (FWHM) at 543 nm was almost 172 nm, which was higher than that reported for CDs [21,30]. Furthermore, the emission peaks position shows no obviously shift and remains at 543 nm when the excitation wavelength ranging from 340 to 440 nm. The photoluminescence wavelength of the CDs is excitation-independent, which is due to the relatively uniform size and surface state of CDs. The quantum yield (QY) of the as-prepared CDs in aqueous solution at room temperature is estimated to be 6.5% using quinine sulfate (0.1 M H_2SO_4 as solvent; QY = 0.54) as a reference.

Furthermore, we investigated the effect of laser power on the PL properties of the produced CDs. Fig. 4(C)–(E) show the PL spectra of the CDs prepared with different laser power of 300 mW, 200 mW and 100 mW, respectively. Each sample was irradiated for 2 h. The emission of the CDs prepared at laser power of 100 mW is mainly in the visible light region with the maximum intensity around 507 nm at an excitation wavelength of 360 nm. The C-dots prepared at laser power of 200 mw showed a maximum emission at 523 nm with 380 nm excitation, while those prepared at 300 mW showed a maximum emission at 541 nm with 380 nm excitation. As a comparison, the maximum fluorescence emission peaks of the C-dots prepared at laser power of 400 mW showed a slightly red-shift and the fluorescence intensity also increases accordingly. Fig. 4(F) shows the maximum fluorescence emission at 380 nm excitation for CDs prepared using different laser power. With increasing the laser power, a red-shift and the fluorescence intensity increased obviously.

Here, we give a brief interpretation about the effects of laser power on the PL spectra of CDs. It's agreed that when femtosecond pulses inject into the graphite powders, Coulomb explosion occurs and a plasma plume with high temperature and high pressure forms. When the plasma plume expands and cools down, a cavitation bubble forms in solution. With the expansion of the bubble, carbon nanoclusters with high surface energy will aggregate into larger NPs. When the temperature and pressure of the bubble drops to a value lower than those of the surrounding solution, the bubble collapses and CDs with reduced size are formed. The CDs come from the bubble undergo modifications due to the condensation of molecular clusters from the solution [20]. Even though the actual mechanism of CD photoluminescence is still an open debate among researchers, there are a huge number of researchers agree that the surface functional groups of CDs play a key role in the effect of its photoluminescence [31–36]. In this study, with the increase of laser power, the chemical reactions between the nanoclusters and the solution molecules are more drastic. Therefore, more surface functional groups, especially nitrogen groups, are connected to the nanoclusters that result in the red-shift of the maximum fluorescence emission peaks.

3.3. *pH sensing*

Due to the uniform size and functional groups on the surface of C dots, the C dots have high compatibility and are miscible in solvents with different pH. Recently, nanoparticle-based ratiometric pH sensors have attracted increasing attention owing to their remarkable advantages, the most important of which being that it is easy to incorporate with diverse dyes on the same nanoparticle to acquire ratiometric fluorescent detection [37,38]. As a nanoparticle-based ratiometric pH sensors, the previously reported pH sensors usually use CDs as diverse dyes' carrier or conjugate CDs with fluorescein isothiocyanate to detect the pH of the solvents. Different from the

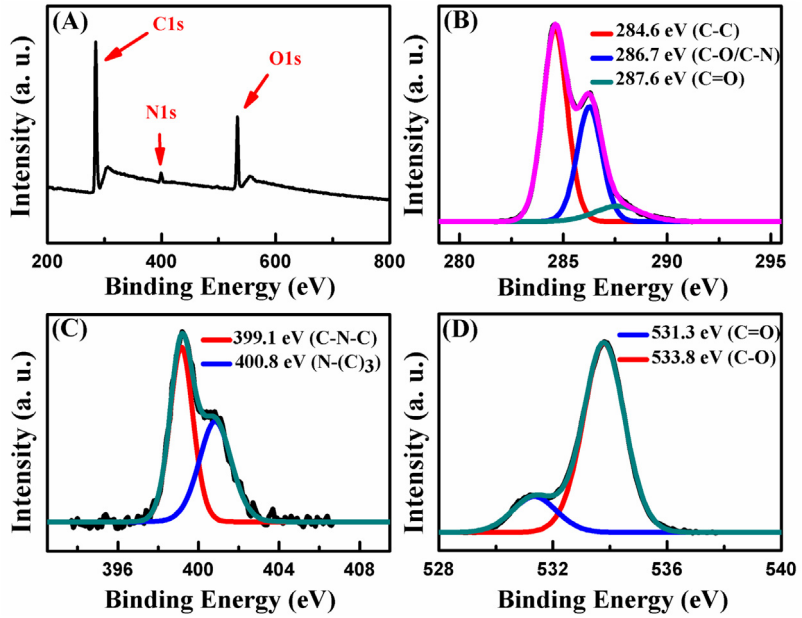

Fig. 3. XPS full scan spectrum (A) and C1s (B), N1s (C), O1s (D) of the CDs.

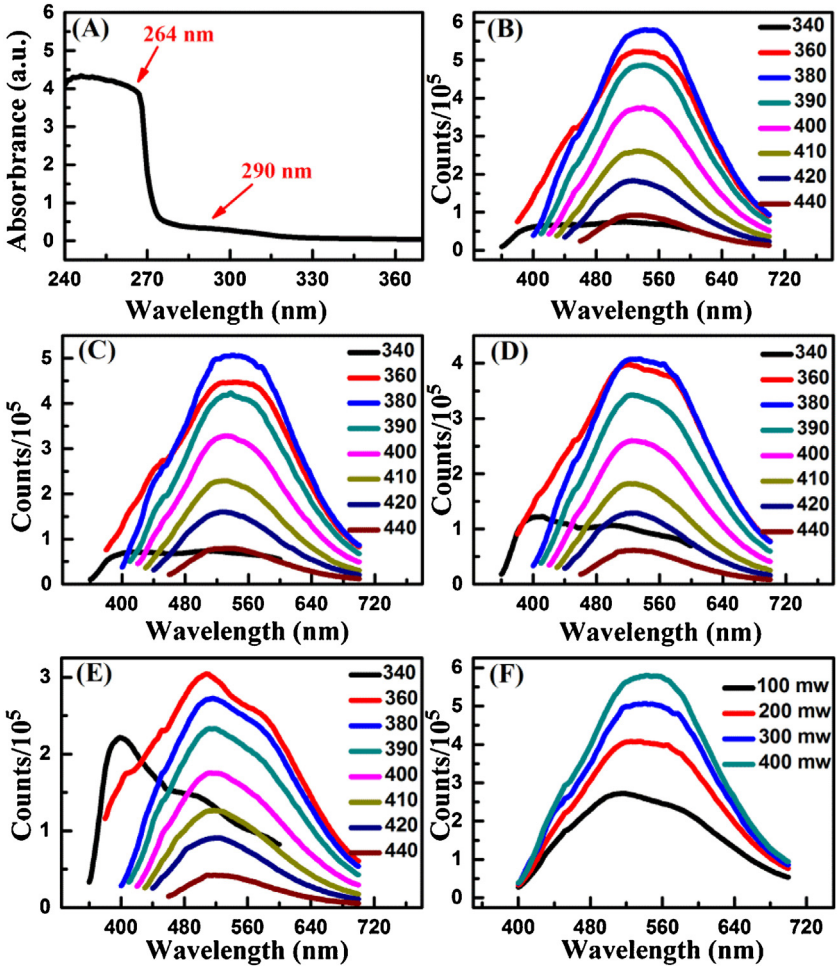

Fig. 4. (A) UV–vis absorption, Fluorescence spectra of the CDs at laser power of (B) 400 mW, (C) 300 mW, (D) 200 mW and (E) 100 mW, (F) Fluorescence spectra of the CDs at different laser power with 380 nm excitation.

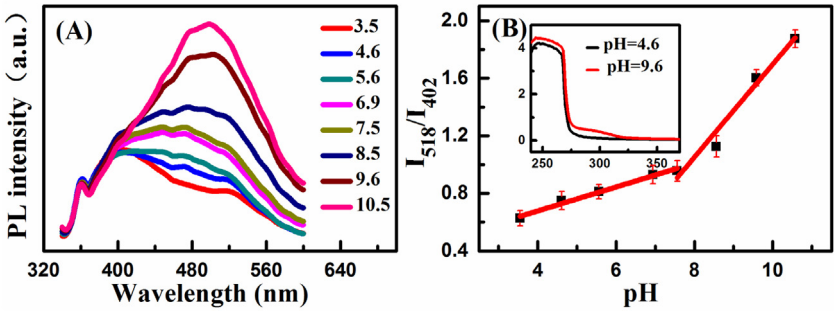

Fig. 5. (A) Fluorescence spectra of the CDs at different pH (B) Fluorescence intensity ratios I_{518}/I_{402} standard curves of the CDs.

previously reported pH sensors, our CDs have an internal reference with a single excitation. As the fluorescence emission of our CDs covers nearly the whole visible light with a single excitation, there are two or more fluorescence intensity references which are used for quantifying the pH value. Thus, there are several independent results can be used to reduce the measurement errors and increase measurement reliability.

Fig. 5(A) shows the fluorescence spectra of the CDs in solvents with different pH. There is a broad emission through a combination of the emission peak at around 402 nm and another emission peak at around 518 nm with a single excitation. The emission peak at around 518 nm increases significantly with increasing pH, while the emission peak at around 402 nm increase little with pH. Thus, there are references to be used for quantifying the pH value which can be determined by measuring the fluorescence intensity ratio of the emission peak at 518 nm to the emission peak at 402 nm in single excitation. The fluorescence intensity ratios standard curves are given in Fig. 5(B). The fluorescence intensity ratios standard curves can be divided into two nearly straight lines with different pH, one is ranged from pH = 3.5 to pH = 7.5 and the other is ranged from pH = 7.5 to pH = 10.5. The UV–vis absorption spectra of the CDs at different pH are given by the inset in Fig. 5(B), the absorption peaks at around 290 nm change significantly with the increasing pH. Because there are multiple oxygen and amine functional groups on the surface of the CDs which can markedly affect its photoluminescence, we think that the second fluorescence emission peak is attributed to the amine functional groups whose activity is easily influenced by the pH of the solution. Because intracellular pH detection plays an important role in cellular processes and the pH variation are closely related to many chemical processes, this newly CDs have huge potential applications in biosensing.

4. Conclusions

In conclusion, excitation-independent fluorescence CDs were synthesized by a one-step pulsed laser ablate the graphite powder in aminotoluene liquid at room temperature. Because there are a huge number of multiple oxygen and amine groups on the surface of the CDs, it have a broad fluorescence emission which can covers nearly the whole visible light with a single excitation. Thus, there are surely two or more fluorescence intensity references which are used for quantifying the pH value. Hence, this work clearly shows that CDs can serve as a promising material to construct practical fluorescent nanosensors which may have a huge potential for quantitatively monitoring the pH in cellular processes and chemical processes.

Acknowledgments

This work was supported the by National Natural Science Foundation of China (Grant No. 61235003, 11674260 and 11474078), the Fundamental Research Funds for the Central Universities, and the collaborative Innovation Center of Suzhou Nano Science and Technology. The work was also supported by the Scientific Research Foundation for the Returned Overseas Chinese Scholars, State Education Ministry. The TEM work was performed at the International Center for Dielectric Research (ICDR), Xi'an Jiaotong University, Xi'an, China. The authors also thank Mr. Ma and Ms. Lu for their help in using TEM.

References

[1] W. Shi, X. Li, H. Ma, A tunable ratiometric pH sensor based on carbon nanodots for the quantitative measurement of the intracellular pH of whole cells, Angew. Chem. 124 (2012) 6538–6541.
[2] L. Albertazzi, B. Storti, L. Marchetti, et al., Delivery and subcellular targeting of dendrimer-based fluorescent pH sensors in living cells, J. Am. Chem. Soc. 132 (2010) 18158–18167.
[3] R.V. Benjaminsen, H. Sun, J.R. Henriksen, et al., Evaluating nanoparticle sensor design for intracellular pH measurements, ACS Nano 5 (2011) 5864–5873.
[4] H. Lu, H. Hao, G. Shi, et al., Optical temperature sensing in β-NaLuF4: Yb3+/Er3+/Tm3+ based on thermal, quasi-thermal and non-thermal coupling levels, RSC Adv. 6 (2016) 55307–55311.
[5] H. Lu, R. Meng, H. Hao, et al., Stark sublevels in Er3+-Yb3+ codoped Gd2 (WO4)3 phosphor for enhancing the sensitivity of luminescent thermometer, RSC Adv. 6 (2016) 57667–57671.
[6] J. Shen, Y. Zhu, X. Yang, et al., Graphene quantum dots: emergent nanolights for bioimaging, sensors, catalysis and photovoltaic devices, Chem. Commun. 48 (2012) 3686–3699.
[7] S.N. Baker, G.A. Baker, Luminescent carbon nanodots: emergent nanolights, Angew. Chem. Int. Ed. 49 (2010) 6726–6744.
[8] X. Michalet, F.F. Pinaud, L.A. Bentolila, et al., Quantum dots for live cells, in vivo imaging, and diagnostics, Science 307 (2005) 538–544.
[9] Y. Xing, Q. Chaudry, C. Shen, et al., Bioconjugated quantum dots for multiplexed and quantitative immunohistochemistry, Nat. Protoc. 2 (2007) 1152–1165.
[10] U. Resch-Genger, M. Grabolle, S. Cavaliere-Jaricot, et al., Quantum dots versus organic dyes as fluorescent labels, Nat. Methods 5 (2008) 763–775.
[11] H. Li, Z. Kang, Y. Liu, et al., Carbon nanodots: synthesis, properties and applications, J. Mater. Chem. 22 (2012) 24230–24253.
[12] L. Cao, X. Wang, M.J. Meziani, et al., Carbon dots for multiphoton bioimaging, J. Am. Chem. Soc. 129 (2007) 11318–11319.
[13] S.T. Yang, L. Cao, P.G. Luo, et al., Carbon dots for optical imaging in vivo, J. Am. Chem. Soc. 131 (2009) 11308–11309.
[14] R.J. Fan, Q. Sun, L. Zhang, et al., Photoluminescent carbon dots directly derived from polyethylene glycol and their application for cellular imaging, Carbon 71 (2014) 87–93.
[15] W. Tan, H. Liu, J. Si, X. Hou, Control of the gated spectra with narrow bandwidth from a supercontinuum using ultrafast optical Kerr gate of bismuth glass, Appl. Phys. Lett. 93 (2008) 051109.
[16] H. Zhang, H. Liu, J. Si, W. Yi, F. Chen, X. Hou, Low threshold power density for the generation of frequency up-converted pulses in bismuth glass by two crossing chirped femtosecond pulses, Opt. Express 19 (2011) 12039.
[17] D. Reyes, M. Camacho, M. Camacho, et al., Laser ablated carbon nanodots for light emission, Nanoscale Res. Lett. 11 (2016) 424.
[18] T. Chen, J. Si, X. Hou, S. Kanehira, K. Miura, K. Hirao, Photoinduced microchannels inside silicon by femtosecond pulses, Appl. Phys. Lett. 93 (2008) 051112.
[19] S.L. Hu, K.Y. Niu, J. Sun, et al., One-step synthesis of fluorescent carbon nanoparticles by laser irradiation, J. Mater. Chem. 19 (2009) 484–488.
[20] V. Nguyen, L. Yan, J. Si, et al., Femtosecond laser-induced size reduction of carbon nanodots in solution: effect of laser fluence, spot size, and irradiation time, J. Appl. Phys. 117 (2015) 084304.

[21] H. Nie, M. Li, Q. Li, et al., Carbon dots with continuously tunable full-color emission and their application in ratiometric pH sensing, Chem. Mater. 26 (2014) 3104–3112.
[22] X. Guo, C.F. Wang, Z.Y. Yu, et al., Facile access to versatile fluorescent carbon dots toward light-emitting diodes, Chem. Commun. 48 (2012) 2692–2694.
[23] P.C. Hsu, H.T. Chang, Synthesis of high-quality carbon nanodots from hydrophilic compounds: role of functional groups, Chem. Commun. 48 (2012) 3984–3986.
[24] X.T. Feng, F. Zhang, Y.L. Wang, et al., Luminescent carbon quantum dots with high quantum yield as a single white converter for white light emitting diodes, Appl. Phys. Lett. 107 (2015) 213102.
[25] Y. Guo, Z. Wang, H. Shao, et al., Hydrothermal synthesis of highly fluorescent carbon nanoparticles from sodium citrate and their use for the detection of mercury ions, Carbon 52 (2013) 583–589.
[26] Y. Guo, Z. Wang, H. Shao, et al., Hydrothermal synthesis of highly fluorescent carbon nanoparticles from sodium citrate and their use for the detection of mercury ions, Carbon 52 (2013) 583–589.
[27] W. Wang, T. Kim, Z. Yan, et al., Carbon dots functionalized by organosilane with double-sided anchoring for nanomolar Hg2+ detection, J. Colloid Interface Sci. 437 (2015) 28–34.
[28] X. Li, S. Zhang, S.A. Kulinich, et al., Engineering surface states of carbon dots to achieve controllable luminescence for solid-luminescent composites and sensitive Be2+ detection, Sci. Rep. 4 (2014) 4976.
[29] Y. Yang, J. Cui, M. Zheng, et al., One-step synthesis of amino-functionalized fluorescent carbon nanoparticles by hydrothermal carbonization of chitosan, Chem. Commun. 48 (2012) 380–382.
[30] L. Hu, Y. Sun, S. Li, et al., Multifunctional carbon dots with high quantum yield for imaging and gene delivery, Carbon 67 (2014) 508–513.
[31] M.J. Krysmann, A. Kelarakis, P. Dallas, et al., Formation mechanism of carbogenic nanoparticles with dual photoluminescence emission, J. Am. Chem. Soc. 134 (2011) 747–750.
[32] V. Nguyen, J. Si, L. Yan, et al., Electron-hole recombination dynamics in carbon nanodots, Carbon 95 (2015) 659–663.
[33] P. Yu, X. Wen, Y.R. Toh, et al., Temperature-dependent fluorescence in carbon dots, J. Phys. Chem. C 116 (2012) 25552–25557.
[34] X. Wen, P. Yu, Y.R. Toh, et al., Intrinsic and extrinsic fluorescence in carbon nanodots: ultrafast time-resolved fluorescence and carrier dynamics, Adv. Opt. Mater. 1 (2013) 173–178.
[35] V. Strauss, J.T. Margraf, C. Dolle, et al., Carbon nanodots: toward a comprehensive understanding of their photoluminescence, J. Am. Chem. Soc. 136 (2014) 17308–17316.
[36] K. Hola, A.B. Bourlinos, O. Kozak, et al., Photoluminescence effects of graphitic core size and surface functional groups in carbon dots: COO- induced red-shift emission, Carbon 70 (2014) 279–286.
[37] H. Sun, A.M. Scharff-Poulsen, H. Gu, et al., Synthesis and characterization of ratiometric, pH sensing nanoparticles with covalently attached fluorescent dyes, Chem. Mater. 18 (2006) 3381–3384.
[38] Y.H. Chan, C. Wu, F. Ye, et al., Development of ultrabright semiconducting polymer dots for ratiometric pH sensing, Anal. Chem. 83 (2011) 1448–1455.